Pergamon

Int. J. Multiphase Flow Vol. 22, No. 2, pp. 403–415, 1996

0301-9322(95)00066-6
0301-9322/96 $15.00 + 0.00

THE VISCOUS RESUSPENSION OF PARTICLES IN AN INCLINED RECTANGULAR FRACTURE

I. MISKIN[1], L. ELLIOTT[1], D. B. INGHAM[1] and P. S. HAMMOND[2]

[1]Department of Applied Mathematical Studies, University of Leeds, Leeds LS2 9JT, U.K.
[2]Schlumberger Cambridge Research Limited, P.O. Box 153, Cambridge CB3 0HG, U.K.

(Received 5 January 1995; in revised form 5 September 1995)

Abstract—It has recently been observed that in laminar shear flows settled particles within a suspension can be resuspended. This phenomena, known as "viscous resuspension", if properly exploited can have a beneficial effect on the process of proppant placement within a hydraulic fracture. By taking advantage of viscous resuspension effects it is possible to entrain particles from a settled bed back into the bulk shear flow which will enable them to be convected deep into the fracture channel and thus avoid the possibility of fracture closure. In practice the sedimentation/resuspension processes usually consist of rigid spherical negatively buoyant particles, which are of approximately equal size and density and do not aggregate, settling at very small particle Reynolds numbers from a suspension comprised of an incompressible Newtonian fluid. In this paper the particle concentration equation is solved initially for a fully developed steady one-dimensional gravity-driven flow down an inclined channel. The problem is then developed by adding a pressure-driven flow across the inclined channel. The concentration, momentum and conservation of mass equations have been solved numerically under a wide variety of operating conditions and initial feed particle concentrations, and typical concentration and velocity profiles at various angles of inclination of the channel and strengths of cross flow are presented.

Key Words: resuspension, channel flow, shear-induced diffusion

1. INTRODUCTION

The phenomena of resuspension is the process by which, in the presence of a shear flow, an initially settled layer of negatively buoyant particles is dragged into the bulk fluid and is convected away. This type of process is usually associated with large Reynolds number flows and turbulence, as discussed in Thomas (1961). However, Gadala-Maria (1979) appear to have been the first to observe that such resuspensions could also occur at small values of Reynolds numbers, say $O(10^{-4})$, for which inertial effects are insignificant and the flow is laminar. During the course of his study, Gadala-Maria (1979) measured the rheological properties of suspensions of coal particles in viscous Newtonian fluids using a parallel plate device. It was found that when the coal suspension was sheared at low shear rates, after having been left overnight, the initial value of the viscosity was significantly lower than that which had been measured the day before. This suggested that the coal particles in the suspension, being heavier than the liquid, had settled overnight. However, when the rate of shear was increased the viscosity was observed to increase and eventually to reach the same value as that measured the day before for a uniform suspension, thereby implying that the settled layer of particles had resuspended.

In a more complete investigation, Leighton & Acrivos (1986) designated this phenomena as "viscous resuspension" and showed that it could be explained in terms of a shear-induced diffusion process, see Leighton & Acrivos (1987), in which the diffusivity resulted from interparticle interactions within a suspension as it is sheared. This diffusion mechanism was found to be quite different from conventional Brownian diffusion, arising from molecular motion, which is negligible for large particles such as those used in the experiments performed by Gadala-Maria (1979) and Leighton & Acrivos (1986, 1987). Since the rate at which these interparticle interactions occur is proportional to the shear rate, $\dot{\gamma}$, and the resulting displacement across streamlines scales with the particle radius, a, then the effective diffusivity from interactions is proportional to $\dot{\gamma}a^2$.

The phenomena of viscous resuspension is of practical importance in many industrial operations. One of the most common processes in industry involves the separation between a particulate phase and the continuous fluid which constitute a particular slurry. Often this is achieved using gravity settling, which is a relatively slow process when particles are small and the fluid is viscous. Thus,

the effect of viscous resuspension could significantly reduce the performance of these settling devices. However, if properly exploited, viscous resuspension can have a positive influence on some industrial operations, such as the process by which proppant particles are placed within a hydraulic fracture in the hydrocarbon industry. When a fracture is created, a fluid containing proppant particles is pumped into it. Ideally, the proppant particles should settle evenly along the entire length of the fracture so that when pumping ceases the fracture is wedged open by the sedimented particles. By taking advantage of viscous resuspension effects it is possible to entrain particles from a settled bed back into the bulk shear flow which will enable them to be convected deep into the fracture channel and thus avoid the possibility of closure.

Dynamical simulations of many-particle systems that account for interparticle effects are computationally expensive and difficult to apply for complex flow geometries which are frequently found in industry. Hence, a continuum model which is based on the fundamental physics of a suspension, but simple enough to be used in flow simulations, would be very valuable. Leighton & Acrivos (1986) devised a simple mathematical model of the resuspension processes observed in a basic Couette type device by considering a balance between the downward flux of particles due to sedimentation and an upward flux due to shear-induced effective diffusion along concentration gradients. A similar model was employed by Schaflinger *et al.* (1990) who investigated theoretically viscous resuspension for two shear flows, specifically a pressure-driven flow in a horizontal channel and a gravity-driven film flow along an inclined plate. More recently, Zhang & Acrivos (1994) developed the model used by Schaflinger *et al.* (1990) to theoretically analyse a more complicated three-dimensional resuspension flow within a horizontal pipe.

The purpose of this paper is to examine theoretically viscous resuspension, using a similar model to that employed by Leighton & Acrivos (1986) and Schaflinger *et al.* (1990), initially for a fully developed steady one-dimensional gravity-driven flow down an inclined channel and then to extend the problem by adding a perpendicular pressure-driven flow across the inclined plane. This latter situation is a reasonable model for proppant flows in inclined fractures provided that the angle of inclination, α, is assumed to be sufficient for entrainment to occur without particles being contained in a stagnant packed bed along the lower surface of the fracture.

2. GRAVITY-DRIVEN FLOW DOWN AN INCLINED CHANNE WITH CROSS FLOW

Consider the flow of a suspension, consisting of uniform spherical particles, down an inclined channel of height $2B$ which is at an angle α to the horizontal when there is a constant pressure gradient applied across the channel, i.e. in the x^*-direction (see figure 1). The volume of flux of clear fluid per unit depth flowing in the x^* and y^*-directions are λQ and Q, respectively, where Q is an adjustable parameter. In this paper we take the region of interest sufficiently far from the inlet regions and down the incline that all the components of the velocity are functions of z^* alone and therefore the z^*-component of velocity is zero. The velocity components are U^* and V^* in the x and y^*-directions, respectively.

As the suspension flows some particles within it will begin to sediment, due to the effect of gravity, while others will resuspend because of the diffusion caused by the shear flow. If steady state is achieved, i.e. the sedimentation flux balances the shear-induced diffusive flux of particles, the flow basically consists of two distinct regions, namely a region of clear fluid above a region of suspension which has a variable concentration (see figure 2). We consider the suspension to consist of rigid spherical negatively buoyant particles, which are of uniform size and density and which do not aggregate, settling at very small Reynolds numbers from a suspension comprised of an incompressible Newtonian fluid. The particle flux due to sedimentation in the z^*-direction is given by

$$N_g = -\phi f(\phi)\left[\frac{2}{9}a^2 \boldsymbol{g}\frac{(\rho_2-\rho_1)}{\mu_1}\right]\cos\alpha \qquad [1]$$

for a rectangular channel inclined at an angle α to the horizontal (see figure 1) where ϕ is the local particle concentration, $\boldsymbol{g}$ is the acceleration due to gravity, a is the particle radius, μ is the viscosity, ρ is the density, $[\frac{2}{9}a^2\boldsymbol{g}(\rho_2-\rho_1)/\mu_1]$ is the dimensional Stokes settling velocity, the subscripts 1 and

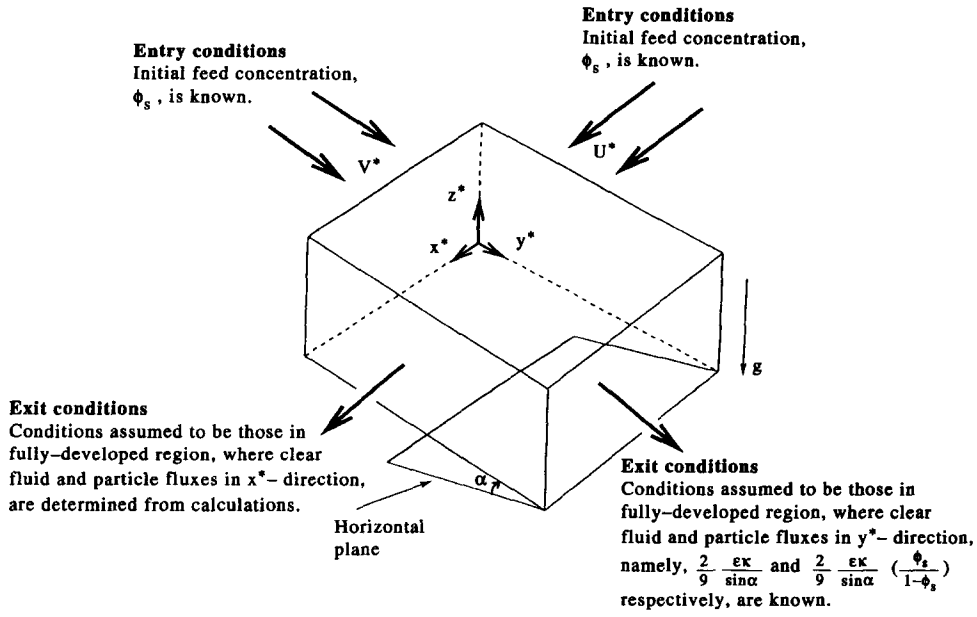

Figure 1. The schematic diagram and coordinate system.

2 refer to the clear fluid and the particle properties, respectively, and $f(\phi)$ is called the hindered settling function. In this work the hindered settling function was chosen to be the same as that used by Leighton & Acrivos (1986), Schaflinger *et al.* (1990) and Zhang & Acrivos (1994), namely,

$$f(\phi) = \frac{1-\phi}{\mu_r} \qquad [2]$$

where μ_r is the relative viscosity between the suspension and the clear fluid and is given by Leighton & Acrivos (1987) as

$$\mu_r = \frac{\mu_m}{\mu_1} = \left[1 + \frac{1.5\phi}{1 - \dfrac{\phi}{\phi_0}}\right]^2 \qquad [3]$$

where ϕ_0 is the volume fraction of particles in the state of close packing and typically takes the value 0.58, see Leighton & Acrivos (1986), and the subscript m denotes the suspension properties. According to Leighton & Acrivos (1987), the particle flux due to shear-induced diffusion can be expressed as

$$\underline{N_s} = -D_c\nabla^*\phi - D_s\nabla^*\dot{\gamma}^* \qquad [4]$$

where the scalars D_c and D_s are dimensional forms of the shear-induced diffusion coefficients and

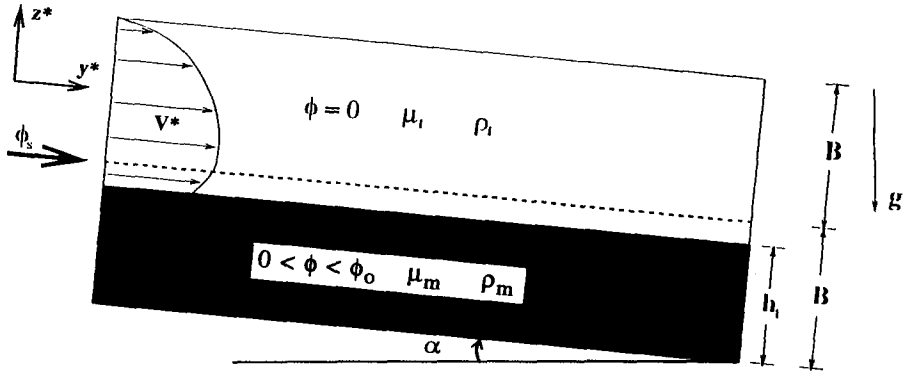

Figure 2. The cross section of the channel in the y–z plane.

$\dot{\gamma}^*$ is the effective shear rate and * denotes dimensional quantities. The dimensionless forms of the coefficients D_c and D_s which are used in this work were given by Phillips *et al.* (1992) as

$$\hat{D}_c \equiv \frac{D_c}{a^2\dot{\gamma}^*} = K_c\phi + K_\mu\phi^2\frac{1}{\mu_r}\frac{d\mu_r}{d\phi}, \quad \hat{D}_s \equiv \frac{D_s}{a^2} = K_c\phi^2 \tag{5}$$

where K_c and K_μ are constants of proportionality which have to be determined exprimentally. In all our calculations, we have taken the values of K_c and K_μ to be 0.43 and 0.65, respectively, i.e. the values as suggested by Phillips *et al.* (1992). Since the region of interest in this paper is sufficiently far from the entrance of the fracture then all quantities are assumed to be dependent on z^*. Hence, from [4] and [5] we have

$$N_s = -K_c\, a^2\left(\phi^2\frac{d\dot{\gamma}^*}{dz^*} + \phi\dot{\gamma}^*\frac{d\phi}{dz^*}\right) - K_\mu\phi^2\dot{\gamma}^*\left(\frac{a^2}{\mu_r}\right)\frac{d\mu_r}{d\phi}\frac{d\phi}{dz^*}. \tag{6}$$

Applying the steady momentum equation in the y^*-direction, i.e. down the inclined plane, within the resuspended region yields

$$\frac{d}{dz^*}\left(\mu_m\frac{dV_m^*}{dz^*}\right) = -(1-\phi)\rho_1 g\sin\alpha - \phi\rho_2 g\sin\alpha \tag{7}$$

which on non-dimensionalization becomes

$$\frac{d\tau_m^y}{dz} = -(1+\epsilon\phi) \tag{8}$$

where

$$\epsilon = \frac{\rho_2 - \rho_1}{\rho_1} \tag{9}$$

is the relative density difference between the solid particles and the clear fluid and all lengths, velocity, shear stresses and pressure scales have been non-dimensionalized with respect to $2B$, $4B^2\rho_1\mu_1^{-1}g\sin\alpha$, $2B\rho_1 g\sin\alpha$ and $2B\rho_1 g\sin\alpha$, respectively. The non-dimensional shear rate and shear stress in the y^*-direction, namely $\dot{\gamma}_m^y$ and τ_m^y, respectively, are defined by

$$\dot{\gamma}_m^y = \frac{dV_m}{dz} = \frac{\tau_m^y}{\mu_r} \tag{10}$$

where μ_r is the relative viscosity between the suspension and the clear fluid, as defined by [3]. Similarly, by applying the steady momentum equation in the resuspended region parallel to the x^*-direction we obtain

$$\frac{d}{dz^*}\left(\mu_m\frac{dU_m^*}{dz^*}\right) = \frac{dp^*}{dx^*} \tag{11}$$

which on non-dimensionalization becomes

$$\frac{d\tau_m^x}{dz} = -K \tag{12}$$

where K is the dimensionless pressure gradient in the x^*-direction and the non-dimensional shear rate and shear stress in the x^*-direction, namely $\dot{\gamma}_m^x$ and τ_m^x, respectively, are defined by

$$\dot{\gamma}_m^x = \frac{dU_m}{dz} = \frac{\tau_m^x}{\mu_r}. \tag{13}$$

Because both the velocity and concentration profiles are fully developed, mass is conserved in both the x^* and y^*-directions. Therefore, the dimensionless equation for the conservation of mass for the clear fluid in the x^*-direction can be written as

$$\int_0^{h_t}(1-\phi(z))U_m(z)\,dz + \int_{h_t}^1 U_1(z)\,dz = \lambda\left(\frac{Q}{Q_0}\right) = \frac{2}{9}\frac{\epsilon\kappa}{\sin\alpha}\lambda \tag{14}$$

where $Q_0 = 8B^3\rho_1\mu_1^{-1}g\sin\alpha$ and κ is the modified Shields number which gives a measure of the ratio between the viscous and buoyancy forces and is given by

$$\kappa = \frac{9}{16}\frac{\mu_1 Q}{B^3 g(\rho_2 - \rho_1)}. \qquad [15]$$

Alternatively, (14) can be written in the form

$$\int_0^1 (1-\phi(z))U(z)\,dz = \frac{2}{9}\frac{\epsilon\kappa}{\sin\alpha}\lambda \qquad [16]$$

since $\phi = 0$ for $z \geqslant h_t$, and h_t is the height above the bottom surface of the channel at which the suspension-clear fluid interface occurs. Similarly, conservation of mass in the y^*-direction gives rise to

$$\int_0^1 (1-\phi(z))V(z)\,dz = \frac{2}{9}\frac{\epsilon\kappa}{\sin\alpha}. \qquad [17]$$

Also, the ratio betwen the flux of solid material flowing down the inclined channel, in the y^*-direction, compared to the corresponding flux of clear fluid flowing in this direction can be written as

$$\int_0^1 \phi(z)V(z)\,dz = \frac{2}{9}\frac{\epsilon\kappa}{\sin\alpha}\left(\frac{\phi_s}{1-\phi_s}\right) \qquad [18]$$

where ϕ_s is the initial feed concentration before the cross flow component of the flow is added, and U and V are the continuous velocity profiles across the whole channel in the x^* and y^*-directions, respectively. Now, because a steady state is assumed to exist, the particle fluxes due to sedimentation and shear-induced diffusion must balance, i.e.

$$N_g + N_s = 0. \qquad [19]$$

By making use of [1], [2], [6] and [19] we obtain

$$\frac{2}{9}a^2 g\phi\frac{1-\phi}{\mu_r}\frac{(\rho_2-\rho_1)}{\mu_1}\cos\alpha + K_c a^2\left(\phi^2\frac{d\dot{\gamma}_m^*}{dz^*} + \phi\dot{\gamma}_m^*\frac{d\phi}{dz^*}\right) + K_\mu\dot{\gamma}_m^*\phi^2\left(\frac{a^2}{\mu_r}\right)\frac{d\mu_r}{d\phi}\frac{d\phi}{dz^*} = 0 \qquad [20]$$

where

$$\dot{\gamma}_m^* = \frac{\tau_m^*}{\mu_m} = \frac{1}{\mu_m}[(\tau_m^{*x})^2 + (\tau_m^{*y})^2]^{1/2}$$

$$= \frac{Q_0}{(2B)^2}\frac{1}{\mu_r}[\tau_m^{x2} + \tau_m^{y2}]^{1/2}. \qquad [21]$$

It should be noted that in the earlier papers, see Leighton & Acrivos (1986) and Schaflinger *et al.* (1990), which deal with shear-induced diffusion, they were limited to unidirectional flows where the diffusion coefficient is proportional to the local shear rate or shear stress. Although the generalization of this result to two and three-dimensional flows is not obvious and needs to be investigated by further experimental studies, it is assumed for simplicity in this paper that the shear-induced diffusion coefficient is proportional to the absolute local shear rate.

By non-dimensionalizing [20], using [21] and then re-arranging we obtain

$$\frac{d\phi}{dz} = -\frac{\frac{2}{9}\epsilon(1-\phi)\cot\alpha + K_c\phi\frac{d}{dz}[\{\tau_m^{x2} + \tau_m^{y2}\}^{1/2}]}{\{\tau_m^{x2} + \tau_m^{y2}\}^{1/2}\left[\frac{(K_\mu - K_c)}{\mu_r}\frac{d\mu_r}{d\phi}\phi + K_c\right]} \qquad [22]$$

which is the particle diffusion equation.

3. SOLUTION PROCEDURE

In order to be able to calculate the velocity and concentration profiles across the entire channel, the system of equations [8], [10], [12], [13], [16]–[18] and [22] is written in the following differential form, i.e.

$$\frac{d\tau^x}{dz} = -K \quad [23]$$

$$\frac{d\tau^y}{dz} = -(1 + c\phi) \quad [24]$$

$$\frac{dU}{dz} = \frac{\tau^x}{\mu_r} \quad [25]$$

$$\frac{dV}{dz} = \frac{\tau^y}{\mu_r} \quad [26]$$

$$\frac{dP_1}{dz} = (1 - \phi)U \quad [27]$$

$$\frac{dP_2}{dz} = (1 - \phi)V \quad [28]$$

$$\frac{dR}{dz} = \phi V \quad [29]$$

$$\frac{d\phi}{dz} = -\frac{\frac{2}{9}\epsilon(1-\phi)\cot\alpha + K_c\phi\frac{d}{dz}\left[\{\tau_m^{x2} + \tau_m^{y2}\}^{1/2}\right]}{\{\tau_m^{x2} + \tau_m^{y2}\}^{1/2}\left[\frac{(K_\mu - K_c)}{\mu_r}\frac{d\mu_r}{d\phi}\phi + K_c\right]} \quad [30]$$

for $0 < z < 1$, where

$$\phi = 0 \quad \text{for} \quad z \geqslant h_t \quad [31]$$

and

$$P_1 = \int_0^z (1-\phi)U\,dz, \quad P_2 = \int_0^z (1-\phi)V\,dz, \quad \text{and} \quad R = \int_0^z \phi V\,dz. \quad [32]$$

The above system of equations has to be solved subject to the following boundary conditions:

$$U = V = P_1 = P_2 = R = 0 \quad \text{at} \quad z = 0 \quad [33]$$

$$U = V = \phi = 0, \quad P_1 = \frac{2}{9}\frac{\epsilon\kappa}{\sin\alpha}\lambda, \quad P_2 = \frac{2}{9}\frac{\epsilon\kappa}{\sin\alpha} \quad \text{and} \quad R = \frac{2}{9}\frac{\epsilon\kappa}{\sin\alpha}\left(\frac{\phi_s}{1-\phi_s}\right) \quad \text{at} \quad z = 1 \quad [34]$$

and were solved by employing a Runge–Kutta Merson method. It should be noted that this problem is well posed since we have eight first-order ordinary differential equations, eleven boundary conditions and three unknown parameters, namely the height above the bottom of the channel at which the suspension–clear fluid interface occurs, h_t, the parameter determining the strength of the cross flow, λ, and the dimensionless pressure gradient in the x^*-direction, K. The numerical method used determines the unknown parameters as well as the solution of the system of equations [23]–[30] given the angle of inclination, α, the Shields number, κ, the initial particle volume fraction, ϕ_s and the relative density difference between the solid particles and the clear fluid, ϵ. However, in the limiting situation when $\lambda = 0$, the system of equations reduces to five first-order ordinary differential equations, seven known boundary conditions and two unknown parameters, h_t and κ or α. In this case we have specified α as known.

4. RESULTS AND DISCUSSION

We will consider the problem for the following two cases:

(i) No cross flow, i.e. when the flow is simply driven by gravity down the inclined plane in the y^*-direction, i.e. $\lambda \equiv 0$.

(ii) Cross flow, i.e. when a pressure-driven flow in the x^*-direction is added to the flow described in case (i), i.e. $\lambda > 0$.

Case (i): $\lambda \equiv 0$

Figure 3(a) and (b) illustrates some typical particle concentration and velocity profiles, respectively, for various values of the Shields number, κ, when $\lambda = 0$, $\phi_s = 0.3$ and $\epsilon = 1$. It should be noted that one can take the angle of inclination, α, or the Shields number, κ, to be the unknown parameter to be determined, in addition to h_t. From figure 3(a) it can be seen that when the angle of inclination is 10°, then $\kappa = 4 \times 10^{-6}$ and the channel becomes almost entirely packed by sediment. As α, and hence κ, which is a measure of the flow rate of clear fluid, increased resuspension occurs and the particles within the resulting suspension layer become less closely packed. Hence the effective viscosity of the suspension layer decreases making it flow more easily. Whilst figure 3(a) displays a decrease in the thickness of the suspension layer with increasing κ, figure 3(b) shows that the corresponding velocity in the suspension layer increases. When the angle of inclination reaches 28°, then $\kappa = 3.1 \times 10^{-2}$ and the sediment layer has almost been totally resuspended, i.e. we observe a constant particle concentration profile with a sudden cut off to zero, as shown in figure 3(a). From figure 3(b) it is observed that as α increases, the magnitude of the maximum velocity, which occurs in the neighbourhood of the suspension–clear fluid interface, decreases. In the case when total resuspension has virtually occurred, i.e. when $\alpha = 28°$, a totally parabolic velocity profile is detected across the channel with the maximum value occurring at the suspension–clear fluid interface.

As ϵ increases then the sedimentation due to gravity becomes more dominant and therefore a larger value of κ is required for total resuspension to occur. Alternatively, as ϵ decreases then gravity becomes less dominant and the situation approaching total resuspension will result at a smaller value of κ. We illustrate this in figure 4 by varying ϵ when the channel is inclined at an angle 18° to the horizontal. It is clearly observed that as the value of ϵ increases we obtain a more concentrated and thicker suspension layer and this indicates that gravity is becoming more important. However, as the value of ϵ decreases then the converse is true, i.e. resuspension becomes more dominant. It should be noted that for very weak flows a convergent solution is difficult to

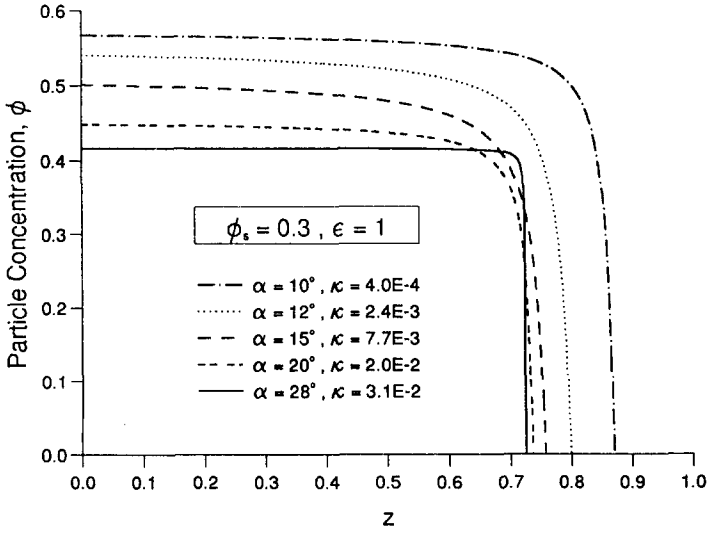

Figure 3(a). The particle concentration, ϕ, as a function of the non-dimensional variable, z, when $\lambda = 0$, $\epsilon = 1$ and $\phi_s = 0.3$ for various angles of inclination, α.

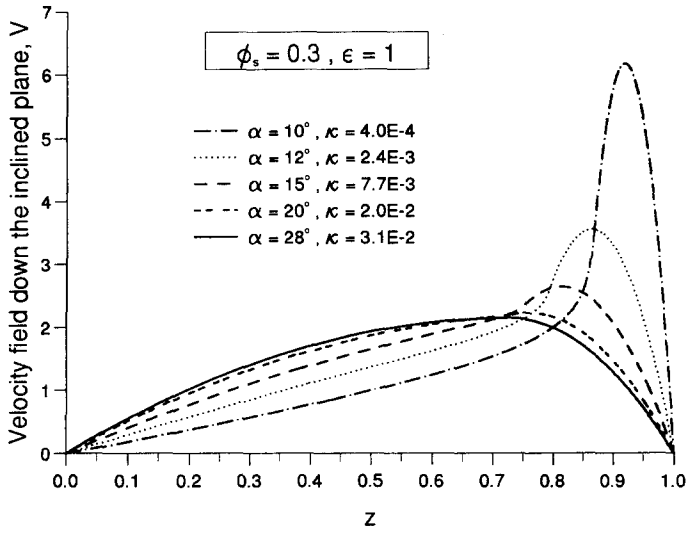

Figure 3(b). The dimensionless y-component of velocity, V, as a function of the non-dimensional variable, z, when $\lambda = 0$, $\epsilon = 1$ and $\phi_s = 0.3$ for various angles of inclineation, α.

obtain since the situation would be approached where a stagnant sediment forms along the lower surface of the channel.

Additionally, it should be pointed out that in the absence of any concentration the present case ($\lambda = 0$) is equivalent to that studied by Schaflinger *et al.* (1990) ($\lambda^{-1} = 0$), with the appropriate external pressure gradient applied. However, any non-zero concentration means that, even for the limiting situation of full resuspension, in this case ($\lambda = 0$) different gravitational forces exist in the clear and the uniform concentration regions. Hence, we can no longer relate the present case to that studied by Shaflinger *et al.* (1990) ($\lambda^{-1} = 0$) where the applied external pressure gradient is constant across the entire channel.

Case (ii): $\lambda > 0$

In order to illustrate the solution procedure, the governing equations [23]–[30] were solved for various values of κ, subject to the boundary conditions [33]–[34], initially, when the channel was inclined at an angle of 18° to the horizontal and the relative density difference between the solid

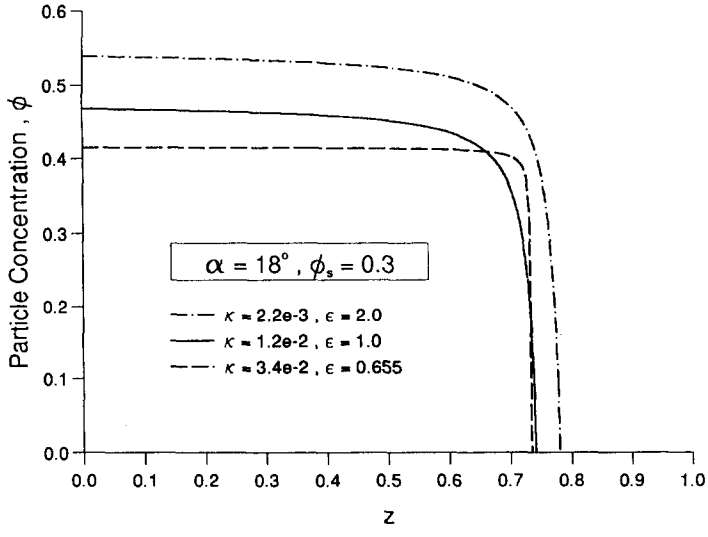

Figure 4. The particle concentration, ϕ, as a function of the non-dimensional variable, z, when $\lambda = 0$, $\alpha = 18°$ and $\phi_s = 0.3$ for various values of ϵ.

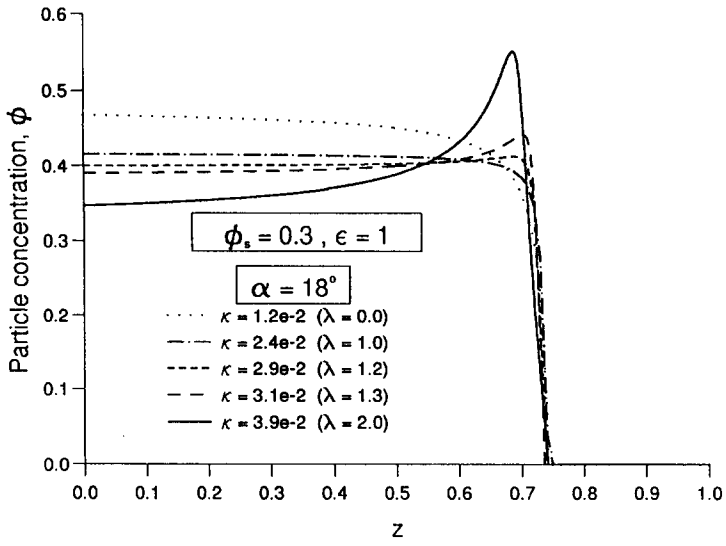

Figure 5. The particle concentration, ϕ, as a function of the non-dimensional variable, z, when $\alpha = 18°$, $\epsilon = 1$ and $\phi_s = 0.3$ for various values of κ.

and fluid fractions, ϵ, was set to unity. The ratio of the flux of solid material to that of clear fluid in the y^*-direction was fixed, for example $\phi_s/(1-\phi_s) = \frac{3}{7}$ when $\phi_s = 0.3$. Across the channel a Poiseuille type flow, subject to varying viscosity with concentration, was set up and the parameter κ, was varied. As κ increases it was found that the value of λ required to maintain the fully developed profiles also increases, i.e. the strength of the cross flow increases. Also, the concentration within the suspension layer decreases and the concentration profiles obtained becomes flatter (see figure 5). This indicates that the limit of total resuspension is being approached. However, it should be noted that as κ increases further, in excess of $\kappa = 2.6 \times 10^{-2}$ at $\alpha = 18°$, then the value of λ slightly exceeds 1.0 (i.e. the rate of flow of clear fluid in the x^*-direction corresponds closely with that in the y^*-direction), and the particle concentration in the outer region of the resuspension zone begins to increase. This observation can be explained by noting that as more clear fluid flows then the magnitude of the shear rate within the suspension increases, but in this case the shear rate has increased sufficiently to enable a positive gradient in concentration to exist.

At this point it is necessary to discuss in some detail the differences in the concentration profiles in case (ii) as the strength of the cross flow increases compared with case (i), when the flow is simply down the channel, as the angle of inclination increases towards its maximum value. In case (i) the limiting situation in which total resuspension is assumed to occur is taken to be the angle of inclination of the channel to the horizontal, α, above which a convergent numerical solution becomes very difficult to obtain. As the angle of inclination of the channel increases, the magnitude of the shear stress in the region just above the lower wall of the channel increases and this results in an increase in the amount of resuspension that is possible. The limiting situation is identified by the existence of a region of constant concentration which extends from the lower wall of the channel to the interface between the suspension and the clear fluid where the value of the concentration changes to zero in an almost discontinuous manner [see figure 3(a)]. Until shortly before the limiting value of the angle of inclination is reached the value of zero shear stress occurs within the clear fluid and the solution of the concentration equation is restricted to a domain which is free of a zero shear stress which would cause a singularity in [30]. However, once the point where the shear stress is zero reaches the edge of the non zero concentration region, it is necessary for the numerical scheme for the concentration equation, i.e. [30], to accommodate this singularity. Obviously the changing position of the singularity and its non-analytical representation makes any attempt at its removal virtually impossible. From [30] it should be emphasized that the point of zero shear stress has to be accompanied by an infinite gradient in the concentration. Hence, numerical difficulties arise when the concentration profiles at large angles of inclination are sought.

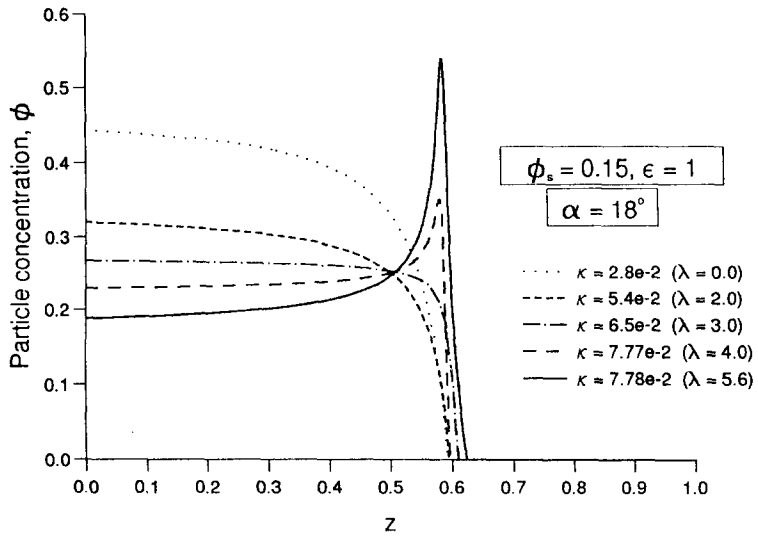

Figure 6. The particle concentration, ϕ, as a function of the non-dimensional variable, z, when $\alpha = 18°$, $\epsilon = 1$ and $\phi_s = 0.15$ for various values of κ.

For case (ii), as in case (i), the shear stress, $\tau_m = (\tau_m^{x2} + \tau_m^{y2})^{1/2}$, increases in the region just above the lower surface of the channel as the angle of inclination, α, and the strengths of flows, namely λQ and Q in the x^* and y^*-directions, respectively, increase, resulting in an increase in the amount of resuspension. However, in this situation, since the shear stress is never zero, more and more material will be resuspended without any breakdown in the numerical method. Hence, for sufficiently large flow rates of clear fluid in the y^*-direction we are able to observe positive gradients in concentration. It should be noted that even for flows where λ is unity, i.e. where the flow rates of clear fluid are equivalent in the x^* and y^*-directions, the corresponding velocity profiles are not identical since hydrodynamic diffusion is a highly non-linear process. Hence, for such flows the

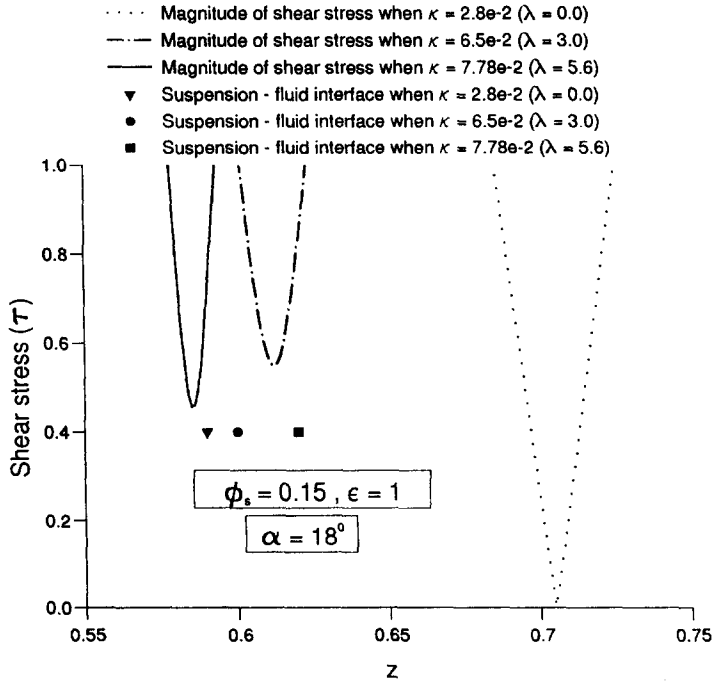

Figure 7. The magnitude of the shear stress, $|\tau|$, as a function of the non-dimensional variable, z, when $\alpha = 18°$, $\epsilon = 1$ and $\phi_s = 0.15$ for various values of κ.

absolute shear within the suspension, τ_m, is non-zero and thus the situation where total resuspension occurs is avoided.

In addition to the above calculations with $\phi_s = 0.3$ and $\alpha = 18°$, further calculations were performed with the value of ϕ_s set to be 0.15. Figure 6 shows the concentration profiles, obtained by solving the system of equations [23]–[30] subject to the boundary conditions [33]–[34], for different values of the parameter κ and it is again observed that a concentration peak forms close to the suspension–clear fluid interface region when the values of κ, and hence λ, are found to be sufficiently large. However, in this case a value of $\kappa = 6.6 \times 10^{-2}$ ($\lambda \approx 3$) was required for a concentration peak to be observed, whereas in the case when $\phi_s = 0.3$ (see figure 5) this situation occurred when $\kappa = 2.6 \times 10^{-2}$ ($\lambda \approx 1$). The reason for this is that for a particular value of κ there are fewer particle collisions when $\phi_s = 0.15$ than for the corresponding case when $\phi_s = 0.3$ since the average particle concentration in the former situation is less. Hence, the flux of particles opposing gravity will be lower when $\phi_s = 0.15$ and in order to obtain a greater migration of particles a larger shear rate is required within the suspension and this can only be achieved with a larger value of κ. Also, it is observed from figure 6 that the concentration peak always occurs close to the suspension–clear fluid interface region. This is because the magnitude of the shear stress is always larger at the bottom of the channel and tends to decrease with height into the region in the neighbourhood close to the suspension–clear fluid interface. To illustrate this more clearly figure 7 shows the variation of the magnitude of the shear stress close to the suspension–clear fluid interface. Thus, more particles migrate from the bottom of the channel, i.e. from the regions of largest shear, and hence this results in a build up of particles close to the suspension–clear fluid interface. In fact, when $\kappa = 7.78 \times 10^{-2}$ ($\lambda = 5.6$) we almost have a region of maximum particle concentration just below the interface (see figure 6). As κ increases further, the numerical scheme employed has great difficulty in obtaining convergent solutions. This occurs because of problems experienced on integrating across the concentration peak where a very large increase in the relative viscosity between the suspension and the clear fluid is present.

By increasing α and κ, the particle concentration peak is observed to occur at a lower values of λ, for example when $\alpha = 18°$, $\epsilon = 1$ and $\phi_s = 0.3$ then with $\kappa = 2.4 \times 10^{-2}$ ($\lambda = 1.0$) no peak has yet occurred (see figure 5), but when $\alpha = 28°$ a considerable concentration peak is present at this value of λ (see figure 8). However, it should be stressed that this now corresponds to $\kappa = 4.5 \times 10^{-2}$. Physically this means that as α increases, then with the volumes of clear fluid flowing in the x^* and y^*-directions approximately the same a higher value of κ is required. When the value of α is increased even further then concentration peaks begin to be observed at progressively smaller values of λ (see figure 9 which shows concentration profiles for various values of κ when $\alpha = 36°$).

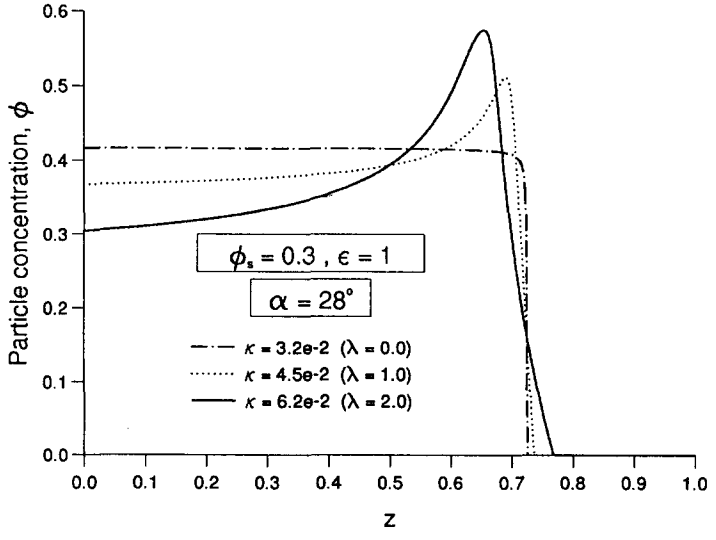

Figure 8. The particle concentration, ϕ, as a function of the non-dimensional variable, z, when $\alpha = 28°$, $\epsilon = 1$ and $\phi_s = 0.3$ for various values of κ.

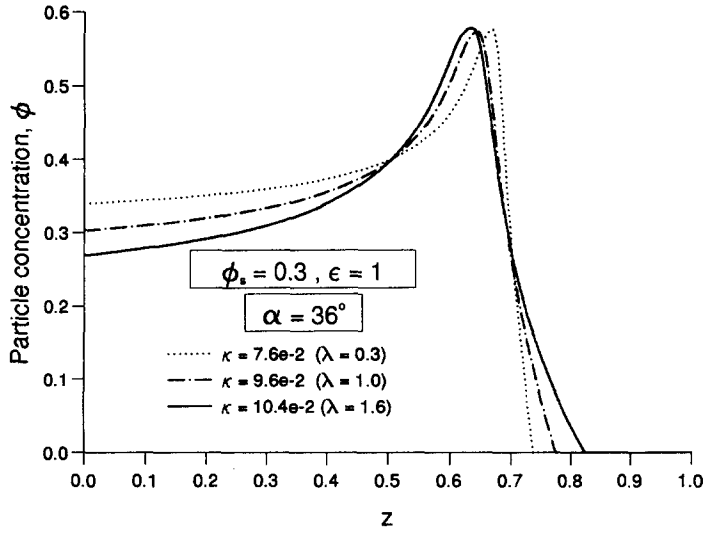

Figure 9. The particle concentration, ϕ, as a function of the non-dimensional variable, z, when $\alpha = 36°$, $\epsilon = 1$ and $\phi_s = 0.3$ for various values of κ.

This is explained simply by the fact that as α increases, a fully developed flow pattern requires higher values of κ, namely, more clear fluid flowing down the channel, resulting in an increase in the shear stress at the walls hence giving rise to a greater resuspension flux of particles. It should again be noted that the numerical technique employed runs into difficulties as the particle concentration reaches its maximum value of 0.58, i.e. the effective viscosity of the suspension tends to infinity when this situation is approached. Thus, for values of α larger than 36° it is very difficult to obtain solutions.

It should be noted that close to the suspension–clear fluid interface $\phi \ll 1$. For this limiting situation the particle diffusion equation [30] can be simplified but, unlike the case considered by Shaflinger *et al.* (1990), it remains analytically intractible.

5. SUMMARY

In this paper we investigated theoretically the viscous resuspension of identical, negatively buoyant, spherical particles, initially for a fully developed steady one-dimensional gravity-driven flow down a rectangular channel and later with a pressure-driven flow added in a direction perpendicular to the original flow. The theoretical approach was based on a model developed by Leighton & Acrivos (1986) in which the net downward flux of particles due to gravity is balanced by a diffusive flux caused by a shear-induced random motion of particles.

For the case with no cross flow, it is shown that as the angle of inclination increases a constant concentration profile is reached within the resuspension layer and the velocity has its maximum value at the particle–clear fluid interface. Thus, the resuspension is restricted due to the existence of a plane on which the shear stress vanishes and hence solutions at larger angles of inclination are unobtainable.

When $\lambda \neq 0$, that is a cross flow is present, then by increasing the flow rate sufficiently in the y^*-direction at a fixed angle of inclination, produces a value for the concentration within a thin layer close to the centre of the channel that approaches the limit maximum packing, namely, $\phi = 0.58$. When the channel is inclined at larger angles to the horizontal, the ratio of the volume of clear fluid flowing in the x^*-direction to that in the y^*-direction at which this maximum packing condition is reached is found to decrease.

When the initial feed concentration, ϕ_s increases the number of particle–particle interactions increases and the value of κ, a measure of flow rate in the y^*-direction, at which the maximum packing condition is reached decreases.

Finally, it is important to point out that our whole analysis has been based upon the generalization of the experimental result stating that the shear-induced diffusion coefficient is

proportional to the absolute shear rate. Since this result has only been verified for simple uni-direction flows it requires further experimental investigation.

REFERENCES

Gadala-Maria, F. A. 1979 The rheology of concentrated suspensions. Ph.D. thesis, Stanford University, CA.

Leighton, D. 1985 The shear-induced migration of particulates in concentrated suspensions. Ph.D. thesis, Stanford University, CA.

Leighton, D. & Acrivos, A. 1986 Viscous resuspension. *Chem. Engng Sci.* **41,** 1377–1384.

Leighton, D. & Acrivos, A. 1987 The shear-induced migration of particles in concentrated suspensions. *J. Fluid Mech.* **181,** 415–439.

Phillips, R. J., Armstrong, R. C., Brown, R. A., Graham, A. L. & Abbott, J. R. 1992 A constitutive equation for concentrated suspensions that accounts for shear-induced particle migration. *Phys. Fluids A* **4,** 30–40.

Schaflinger, U., Acrivos, A. & Zhang, K. 1990 Viscous resuspension of a sediment within a laminar and stratified flow. *Int. J. Multiphase Flow* **16,** 567–578.

Thomas, D. G. 1961 Transport characteristics of suspensions. *AIChE J.* **7,** 423–430.

Zhang, K. & Acrivos, A. 1994 Viscous resuspension in fully developed laminar pipe flows. *Int. J. Multiphase Flow* **20,** 579–591.